Environmental Technology & Innovation 39 (2025) 104269

Contents lists available at ScienceDirect

Environmental Technology & Innovation

journal homepage: www.elsevier.com/locate/eti

Biochar-based controlled-release ammonium phosphate fertilizer: Synthesis and impact on soil nutrient dynamics, wheat growth, and yield under controlled conditions

Sebastián Meier [a,b], Pedro M. de Souza Campos [a], Rubén Palma-Millanao [c], Natalia Rojas [d], María-Eugenia González [e,f], Sigrid Muñoz [g], Gabrijel Ondrasek [h], Khan Naser [i], Juan Hirzel [j], Alex Seguel [k,*]

[a] Instituto de Investigaciones Agropecuarias. INIA Carillanca, Casilla Postal 929, Temuco, Chile
[b] Escuela de Agronomía, Facultad de Ciencias, Ingeniería y Tecnología, Universidad Mayor, Temuco, Chile
[c] Instituto de Investigaciones Agropecuarias INIA La Cruz, Chorrillos 86, La Cruz, Región de Valparaiso, Chile
[d] Vicerrectoría de Investigación y Postgrado, Universidad de La Frontera, Temuco, Chile
[e] Departamento de Ingeniería Química, Facultad de Ingeniería y Ciencias, Universidad de La Frontera, Temuco, Chile
[f] Scientific and Technological Bioresources Nucleus-BIOREN, Universidad de La Frontera, Temuco, Chile
[g] Carrera de Agronomía, Facultad de Ciencias Agropecuarias y Medioambiente, Universidad de La Frontera, Temuco, Chile
[h] Faculty of Agriculture, University of Zagreb, Svetosimunska c. 25, Zagreb 10000, Croatia
[i] School of Chemical Engineering, University of Adelaide, Adelaide, SA 5000, Australia
[j] Instituto de Investigaciones Agropecuarias. INIA Quilamapu, Av. Vicente Méndez 515 Chillán, Chile
[k] Departamento de Ciencias Agronómicas y Recursos Naturales, Facultad de Ciencias Agropecuarias y Medioambiente, Universidad de La Frontera, Temuco, Chile

ARTICLE INFO

Keywords:
Biochar-supported controlled-release fertilizer
Nitrogen and phosphorus use efficiency
Nutrient recovery
Sustainable agriculture

ABSTRACT

Current agricultural practices prioritize increasing crop yields through extensive fertilizer use. However, overreliance on nitrogen (N) and phosphorus (P) fertilizers has led to environmental degradation, including eutrophication and inefficient nutrient use, raising sustainability concerns. This study aims to develop a biochar-supported controlled-release fertilizer (BAPF) containing N and P, and evaluate its impact on soil nutrient dynamics, nutrient recovery, plant growth, and yield. BAPF was synthesized by impregnating biochar derived from oat hulls with urea and diammonium phosphate. An eight-week soil incubation experiment compared nutrient release dynamics between BAPF, conventional fertilizers (CF), oat hull biochar (OHB), and a control (CT). BAPF demonstrated consistent nutrient release, maintaining higher N and P availability over time than CF. By day 60, total N concentration in the BAPF treatment was 6 % higher than CF, while P availability was consistently 20 % higher. BAPF also exhibited lower ammonification rates compared to unfertilized treatments, while nitrification rates were 2.6 times greater compared to OHB and CT, demonstrating enhanced nitrogen conversion efficiency. In a greenhouse trial using spring wheat as a model plant, BAPF improved growth, nutrient uptake, and grain yield compared to CF, OHB, and CT. Total biomass and grain yield increased by approximately 15 % relative to CF, and nutrient recovery rates were significantly higher, with N apparent recovery (ARN) of 55.0 % compared to 36.5 % for CF. Additionally, the apparent P recovery rose from 8.9 % in CF to 18.5 % in BAPF. The findings suggest that BAPF improves nutrient use efficiency and enhances

* Corresponding author.
E-mail address: alex.seguel@ufrontera.cl (A. Seguel).

https://doi.org/10.1016/j.eti.2025.104269
Received 29 November 2024; Received in revised form 5 March 2025; Accepted 11 May 2025
Available online 14 May 2025

grain productivity compared to conventional methods. Its controlled-release properties lead to longer nutrient availability, better nutrient recovery, and increased crop productivity, even in high P-fixing soils. Therefore, BAPF offers an effective alternative to reduce reliance on synthetic fertilizers, enhancing sustainability in agricultural systems.

1. Introduction

Global agriculture faces the dual challenge of increasing crop yields and improving nutritional quality while minimizing environmental impacts and reducing costs (Yang et al., 2024). Since the Green Revolution, global crop yields have increased due to advancements in plant breeding and cultivation technologies (Vandamme et al., 2016). However, this progress has depended mainly on the extensive use of inorganic fertilizers, particularly nitrogen (N) and phosphorus (P) (Wang et al., 2022). This reliance raises significant concerns regarding these practices' long-term sustainability and resource use efficiency in agricultural systems.

Nitrogen is an essential nutrient for plant growth, playing a critical role in several physiological and biochemical processes, including photosynthesis, protein synthesis, DNA replication, and enzyme activation (Zayed et al., 2023). Similarly, P is crucial for energy transfer and genetic processes in plants, as it is a component of nucleic acids, ATP, and membrane phospholipids (White and Brown, 2010). In agriculture, both N and P are central to promoting crop growth, enhancing the development of vegetative and reproductive structures, and ultimately increasing biomass production and yields (Anas et al., 2020). In addition, these nutrients also influence the nutritional quality of crops, including protein content and the accumulation of essential micronutrients (Khalid et al., 2023). The agronomic importance of N and P often leads farmers to apply excessive amounts of fertilizers to maximize yields (Cormier et al., 2016). However, this practice comes with significant environmental consequences, such as eutrophication, soil acidification, greenhouse gas emissions, and the degradation of both terrestrial and aquatic ecosystems (Galloway et al., 2014). The environmental impacts ultimately threaten the sustainability of agricultural production. An important issue with conventional fertilizers is their soil nutrient retention inefficiency (Dimin et al., 2014). Mineral forms of N and P are often not retained long enough for plants to fully utilize them, leading to substantial nutrient losses or fixation (Ciampitti and Vyn, 2014). Over half of the applied N is lost through leaching and volatilization as ammonia and nitrous oxide gases, while up to 90 % of applied P fertilizer becomes unavailable to plants due to soil fixation, particularly in soils with high P-fixing capacities like andisols (López-Arredondo et al., 2014; Martínez-Dalmau et al., 2021). These inefficiencies contribute to economic losses for farmers and degrade the environment (Anas et al., 2020).

A promising approach to addressing these challenges is the development of "smart fertilizers" with controlled nutrient-release mechanisms, which minimize nutrient losses and improve nutrient recovery by crops (Calabi-Floody et al., 2018). One such material that has gained attention is biochar (Bc), a carbon-rich product derived from the pyrolysis of organic materials. The Bc is an attractive matrix for developing controlled-release fertilizers due to its porous structure, high surface area, and capacity to retain nutrients, which can improve nutrient use efficiency (Lehmann and Joseph, 2009). Studies have demonstrated that Bc not only enhances soil nutrient exchange capacity but also promotes microbial activity (Gul and Whalen, 2016; Xu et al., 2014) improves water retention (Atkinson, 2018; González et al., 2015), and serves as a carrier for delivering nutrients such as N and P (El Sharkawi et al., 2018). These properties make Bc a strong candidate for mitigating nutrient losses and improving fertilizer efficiency, particularly in agricultural soils prone to nutrient fixation. Previous studies have demonstrated that combining Bc with N fertilizers can effectively modify soil N dynamics, reducing losses through leaching and volatilization(Güereña et al., 2013; Li et al., 2018a; Saha et al., 2018). Similarly, Bc is impregnated with phosphorus sources, which shows the ability to release P more gradually while maintaining nutrient availability comparable to conventional fertilizers (Liang et al., 2014). Phosphate impregnation into the Bc structure facilitates controlled P-release, increases carbon stability, and enhances retention within biochar, optimizing its role as a soil amendment (Carneiro et al., 2018; Zhao et al., 2016).

Despite significant advances in biochar-based controlled-release systems, most studies have focused solely on N release, with limited research addressing the simultaneous incorporation of N and P into BC matrices (Nayak et al., 2025; Pereira et al., 2022). A dual-nutrient formulation can substantially improve nutrient use efficiency by providing a balanced and sustained release of N and P, which is particularly crucial in P-fixing soils where continuous nutrient availability is essential for optimal plant growth and yield (Cui et al., 2022; Gao et al., 2022)

This study aims to develop a biochar-based controlled-release fertilizer (BAPF) that simultaneously delivers N and P to agricultural soils. The objectives are to assess the nutrient release dynamics of BAPF in soil, evaluate its impact on plant growth, nutrient uptake, and grain yield, and compare its performance with conventional fertilization method. It is hypothesized that BAPF enhance nutrient retention, regulate nutrient release, and improve crop productivity while minimizing nutrient losses. This dual-nutrient approach distinguishes this study from previous research, which has primarily focused on the controlled release of a single nutrient (Nayak et al., 2025, 2024; Pereira et al., 2022). Ultimately, this research seeks to contribute to more sustainable nutrient management practices, addressing the inefficiencies of conventional fertilizers and improving both agricultural productivity and environmental sustainability.

2. Materials & methods

Three independent experiments were conducted to evaluate the effectiveness of a biochar-based controlled-release ammonium phosphate fertilizer (BAPF) on soil nutrient release dynamics and its role in plant growth, nutrient uptake, and grain yield. The first experiment involved the synthesis of BAPF by impregnating oat hull biochar (OHB) with urea and diammonium phosphate, followed by a comparative analysis of its physical and chemical properties against the original OHB. The second experiment assessed the changes in N and P dynamics in soil after BAPF application, comparing its performance with conventional fertilization (CF), OHB alone, and an unfertilized control (CT) during an eight-week soil incubation under controlled conditions. The third experiment evaluated the agronomic effectiveness of BAPF for plant growth and nutrient uptake in greenhouse conditions, using wheat as the model plant. Detailed methodologies for each experiment are provided below.

2.1. Synthesis and physicochemical characterization of biochar-based controlled-release ammonium phosphate fertilizer (BAPF, Experiment 1)

2.1.1. Biochar production

Oat hull biochar (OHB) was synthesized at Universidad de La Frontera's Center for Waste Management and Bioenergy. Before initiating the process, the pyrolyzer was purged with N_2 gas to displace air. The temperature gradually increased at a rate of 3.6°C per minute until reaching 300°C, a temperature chosen to preserve functional groups in the Bc structure and optimize yield (Tomczyk

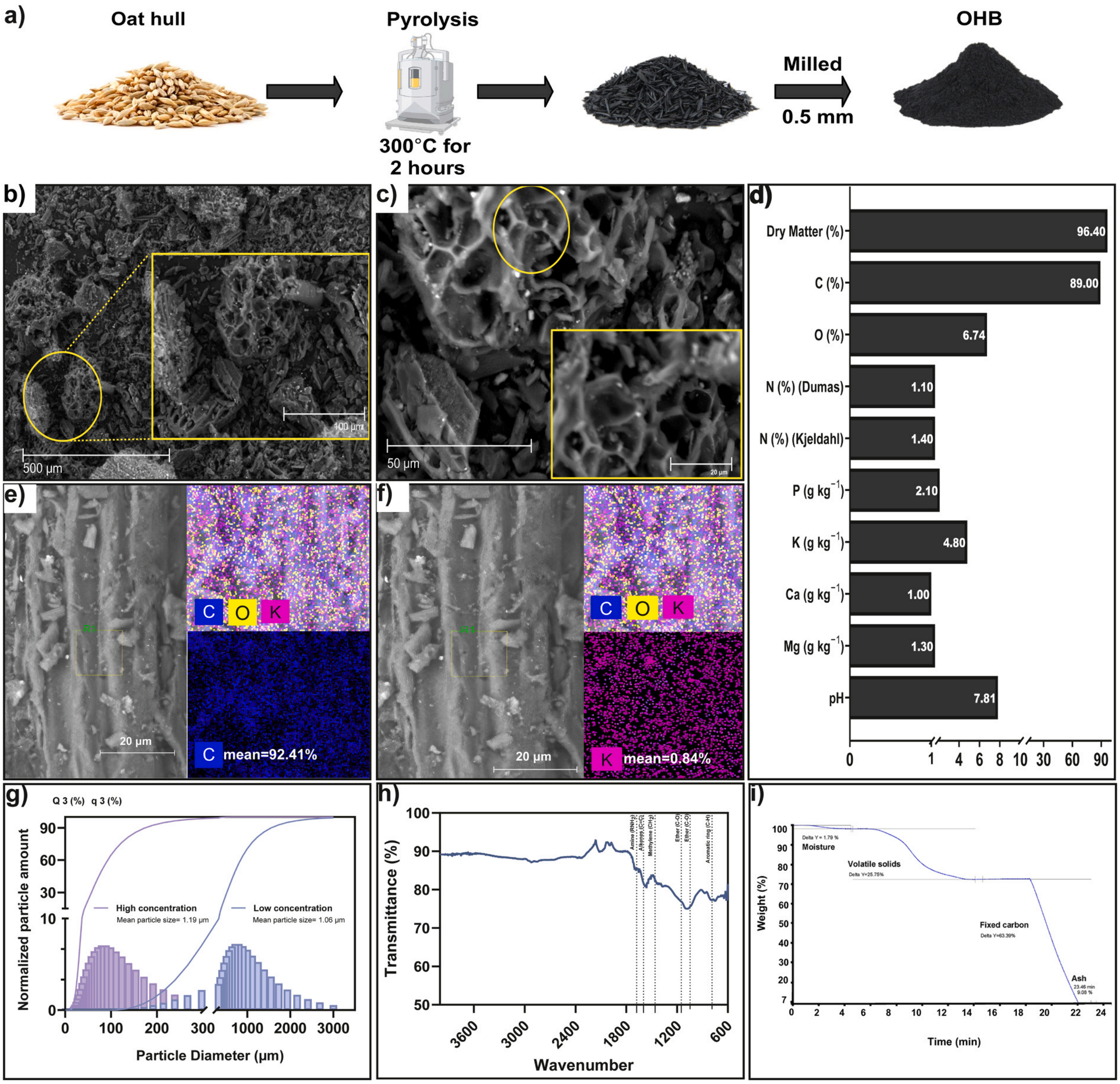

Fig. 1. Preparation and physiochemical characterization of oat-derived biochar (OHB) a) Schematic representation of the preparation of OHB; b), c) Scanning electron microscopy (SEM) images; d) Chemical composition analysis; e, f) Energy-dispersive X-ray spectroscopy (EDS) with elemental mapping of carbon (e) and potassium (f); g) Particle size distribution; h) Fourier-transform infrared spectroscopy (FTIR); i) Thermogravimetric analysis (TGA).

et al., 2020). After pyrolysis, the OHB was allowed to cool to room temperature in a sealed stainless-steel container to prevent exposure to oxygen (Fig. 1a).

2.1.2. Preparation of the BAPF

The OHB was milled and sieved through a 0.5 mm mesh (100-mesh sieve). Dry OHB (4 % moisture content) was impregnated with a mixture of diammonium phosphate (DAP; Productos Químicos Company, Santiago, Chile) and granulated urea (46 % N, Sociedad Química y Minera de Chile S.A.). The N and P contents were adjusted using a modified method from El Sharkawi et al. (2018) and González et al., (2015). Several ratios of Bc, and fertilizers were tested (data not shown), and the optimized formulation was determined to consist of OHB, DAP, urea, and distilled water in a weight ratio of 1:1.25:1.25:1. The mixture was processed in a 5 L electric reactor (Tefal, CY505E30, France) under fume hood containment at 100 °C and 1.0 bar pressure (Fig. 2a). The components were mixed into a uniform paste and evenly distributed within the vessel. Following a 10-minute heating period, the paste was stirred continuously to prevent solidification, then cooled and dried at 25 °C for 24 hours. The resulting product, designated as Biochar-Based Controlled-Release Ammonium Phosphate Fertilizer (BAPF), exhibited particle sizes ranging from 2 to 4 mm and was stored for future use.

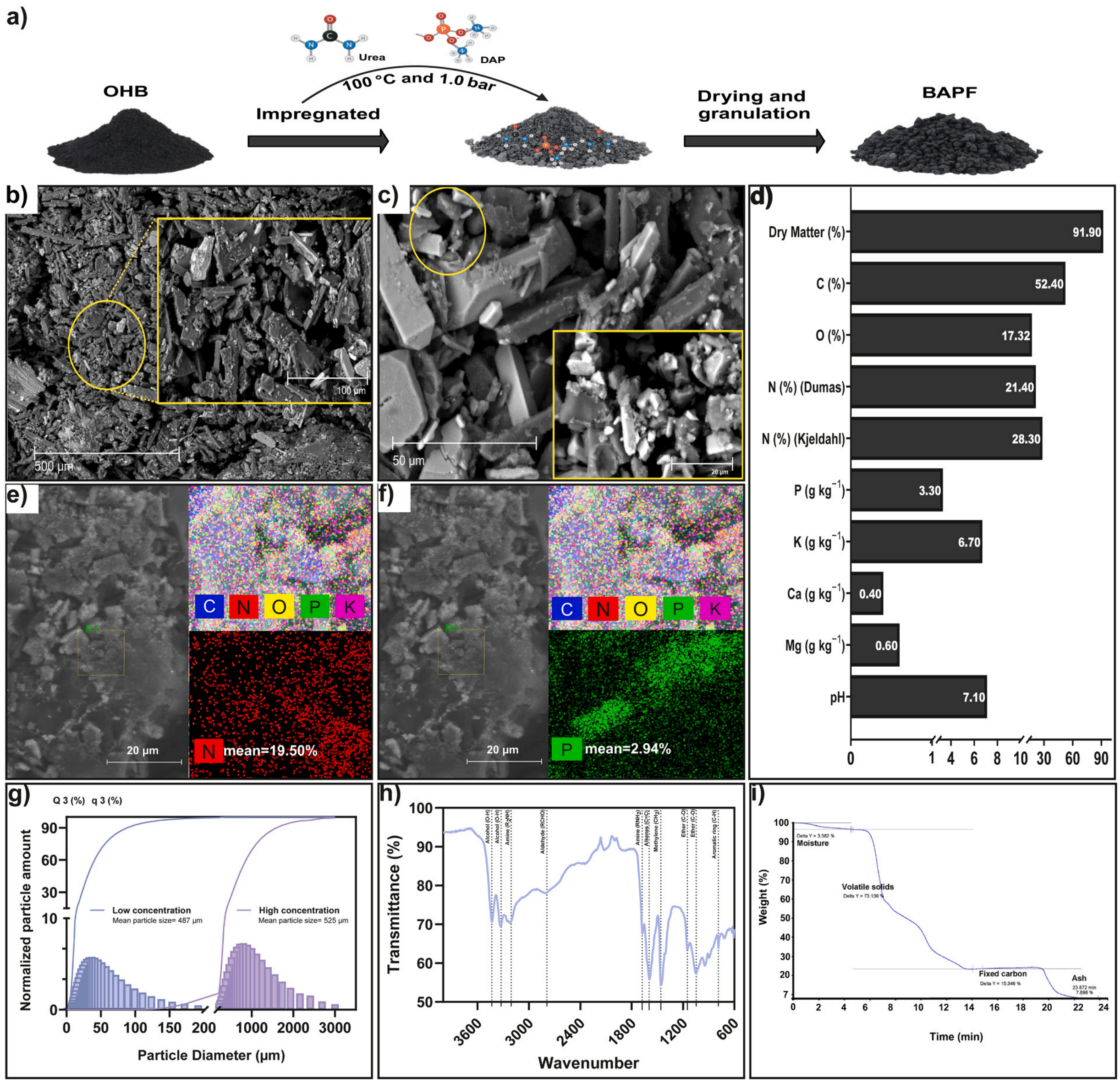

Fig. 2. Synthesis and physiochemical characterization of biochar-based controlled-release N and P fertilizer a) Schematic representation of the preparation of BAPF by impregnating OHB with inorganic fertilizers; b), c) Scanning electron microscopy (SEM) images; d) Chemical composition analysis; e, f) Energy-dispersive X-ray spectroscopy (EDS) with elemental mapping of nitrogen (e) and phosphorus (f); g) Particle size distribution; h) Fourier-transform infrared spectroscopy (FTIR); i) Thermogravimetric analysis (TGA).

2.1.3. Biochar and BAPF characterization

The effectiveness of the impregnation process was evaluated using multiple physicochemical methods, including scanning electron microscopy (SEM), particle size distribution (PSD), thermogravimetric analysis (TGA), energy-dispersive X-ray spectroscopy (EDX), Fourier-transform infrared (FTIR) spectroscopy, and chemical composition analysis.

The morphology of OHB and BAPF was analyzed using SEM (JSM 6380LV microscope, JEOL, USA). PSD was analyzed using a Shimadzu SALD-3101 DRY laser diffraction particle size analyzer (Kyoto, Japan) under dry mode using compressed air to prevent agglomeration. The refractive index was 2.00–0.10i (optimized for Bc), with four signal accumulations per count, a two-second measurement interval, and 64-time signal averaging to enhance accuracy.

Thermogravimetric analysis (TGA) was conducted using a PerkinElmer STA 6000 thermal analysis system (Waltham, Massachusetts, USA). Samples (∼20 mg) were heated from 30 °C to 120 °C at 50 °C/min and held for 3 minutes to remove moisture. Subsequently, the temperature was increased to 950 °C at 100 °C/min under a constant nitrogen flow of 100 mL/min to decompose volatile matter. After cooling, the samples were reheated to 800 °C for 3 minutes to determine the fixed carbon and ash content.

FTIR spectroscopy was used to analyze surface functional groups, employing an Agilent Cary 630 FTIR spectrometer (Santa Clara, USA). The FTIR spectrum was recorded with 64 scans per point and a resolution of 2 cm^{-1}, covering wave numbers from 4000 to 500 cm^{-1}.

The chemical composition analysis of both materials included pH determination (1:5) using a Thermo-Orion 3 Star pH meter. A CN elemental analyzer quantified Total N and Carbon (CE Instruments EA 1108). N content was also evaluated via the Kjeldahl method to

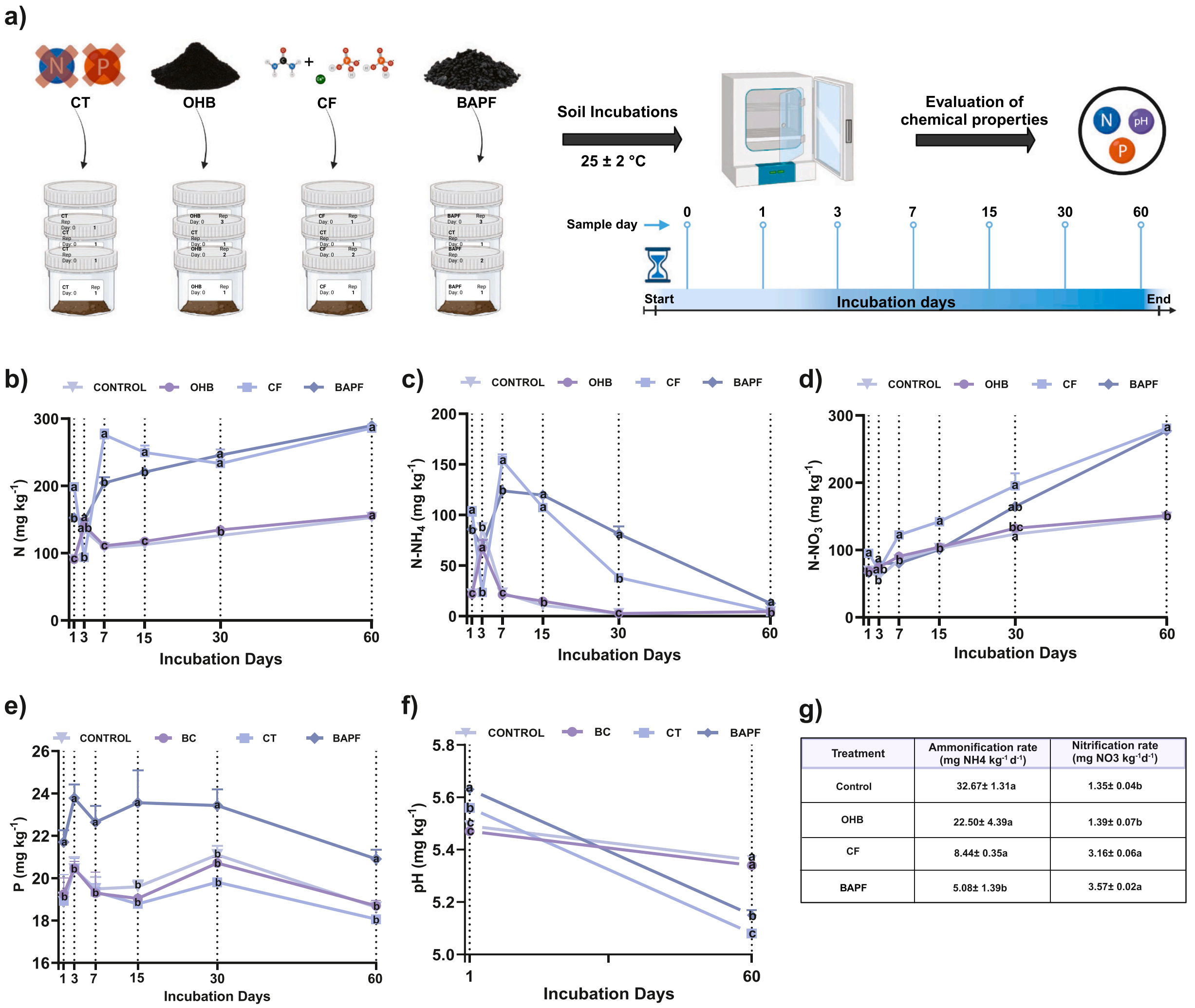

Treatment	Ammonification rate (mg NH4 kg^{-1} d^{-1})	Nitrification rate (mg NO3 $kg^{-1}d^{-1}$)
Control	32.67± 1.31a	1.35± 0.04b
OHB	22.50± 4.39a	1.39± 0.07b
CF	8.44± 0.35a	3.16± 0.06a
BAPF	5.08± 1.39b	3.57± 0.02a

Fig. 3. a) Experimental setup for soil incubation with control (CT) treatments, oat hull-derived biochar (OHB), conventional fertilization (CF), and biochar ammonium phosphate fertilizer (BAPF). Incubation was conducted for 60 days with seven sampling points; b) Changes in total nitrogen (N) throughout incubation; c) Evolution of ammonium nitrogen (N-NH_4^+) during incubation; d) Evolution of nitrate nitrogen (N-NO_3^-) during incubation; e) Evolution of phosphorus (P) during incubation; f) Changes in soil pH from the start to the end of incubation; g) Ammonification and nitrification rates under different treatments (OHB, CF, biochar ammonium phosphate fertilizer, CT).

ensure accurate and comprehensive N quantification. The total phosphorus, potassium, calcium, magnesium, and sulfur concentrations were measured using methodologies described by Sadzawka et al. (2006). Additional carbon, oxygen, and potassium analysis was quantified using EDX with a Quantax XFlash (Bruker, Germany) coupled to the JSM 6380LV SEM.

2.2. Effect of the BAPF on the soil's N and P dynamics (experiment 2)

The impact of BAPF on soil N and P dynamics was evaluated through soil incubations conducted under controlled environmental conditions (Fig. 3a). An agricultural volcanic soil with a silty loam texture (Barros Arana series, medial, mesic, typical Hapludand; CIREN, 2002) was collected in Southern Chile (39°06′S, 72°41′W). The soil was chemically analyzed and physically characterized following procedures described by Sadzawka et al., (2006) and Sandoval et al. (2012) (Table 1).

The soil incubation experiment employed four treatments: (1) Control (CT) with no added fertilization, (2) OHB, (3) conventional fertilization (CF), and (4) BAPF. The N applied to CF and BAPF was equivalent to 200 kg N per hectare across treatments. For CF, urea and triple superphosphate were used as sources of N and P, respectively. OHB was applied in the same amount (weight-to-weight) as BAPF. Since BAPF contained approximately 3 % P, the same amount was added to CF to match the targeted P dosage.

Soil samples (100 g each) were homogenized and placed into plastic jars (0.25 L capacity). The samples were moistened to 60 % of their water-holding capacity and incubated in darkness at 25 ± 2 °C for eight weeks using an incubator (FOC 225E, Velp Scientifica, Usmate, Italy). To allow gas exchange, the jars were opened weekly for one hour, and soil moisture was adjusted to maintain consistent conditions throughout the incubation period. The jars were arranged in a randomized complete block design (RCBD) to minimize positional effects within the incubator. Air circulation within the chamber was maintained to ensure uniform environmental conditions across all samples.

Destructive sampling occurred at 0, 1, 3, 7, 15, 30, and 60 days, with three replicates selected per treatment at each time point. This resulted in 12 experimental units per sampling time and 72 units overall. Soil chemical properties were analyzed at each sampling point following Sadzawka et al. (2006). Available soil N (NO_3^--N and NH_4^+-N) was extracted with 2 M KCl and determined by colorimetry using a Skalar autoanalyzer. Available P (Olsen) was extracted with 0.5 M $NaHCO_3$ and determined using the ascorbic acid-molybdate method. Soil pH was quantified only on days 1 and 60 using a 1:2.5 soil-to-water solution ratio with a pH electrode.

Net ammonification (NammR) and nitrification (NnitR) rates were calculated using NH_4^+-N and NO_3^--N concentrations as outlined by Thangarajan et al., (2013):

$$N_{ammR} = (N_{af} - Nai)/(af - ai) \quad (1)$$

Where: N_{ammR}: Net ammonification rate (mg N kg^{-1} soil d^{-1}), N_{af}: Peak NH_4^+-N concentration (mg NH_4^+-N kg^{-1} soil), N_{ai}: Initial NH_4^+-N concentration (mg NH_4^+-N kg^{-1} soil); af: Time of peak NH_4^+-N concentration (days) ai: Initial sampling time (days)

$$N_{nitR} = (N_{nf} - N_{ni})/(nf - ni) \quad (2)$$

Table 1
Chemical and physical analyses of the soil.

Parameter	Value
pH (water)	5.7
pH ($CaCl_2$)	5.0
Organic matter (%)	18.1
Nitrate (N-NO_3) (mg kg^{-1})	8.2
Ammonium (N-NH_4) (mg kg^{-1})	58.6
P (Olsen) (mg kg^{-1})	24
K (mg kg^{-1})	242
Ca (cmol(+) kg^{-1})	7.35
Mg (cmol(+) kg^{-1})	1.2
K (cmol(+) kg^{-1})	0.62
Na (cmol(+) kg^{-1})	0.11
Sum of base cations (cmol(+) kg^{-1})	9.28
Al (cmol(+) kg^{-1})	0.50
CICE (cmol(+) kg^{-1})	9.98
Al Saturation (%)	7.02
B (mg kg^{-1})	0.5
Cu (mg kg^{-1})	2.0
Zn (mg kg^{-1})	1.3
Al extractable (mg kg^{-1})	714
Ca/Mg relation	6.13
Relation K/Mg	0.52
Electrical conductivity (mS/cm)	0.070
Textural classification	Silty Loam
Field capacity (1/3 atm) (%wt%wt)	74.83
Permanent wilting point (15 atm) (%wt%wt)	50.01
Humidity retention (1/3–15 atm) (%wt%wt)	24.82
Bulk density (mg/m^3)	0.73

Where: N_{nitR}: Net nitrification rate (mg N kg^{-1} soil d^{-1}); N_{nf}: Peak NO_3^--N concentration (mg NO_3^--N kg^{-1} soil); N_{ni}: Initial NO_3^--N concentration (mg NO_3^--N kg^{-1} soil); nf: Time of peak NO_3^--N concentration (days); ni: Initial sampling time (days)

2.3. Effect of BAPF application on plant growth, nutrient uptake, and grain yield (experiment 3)

The impact of BAPF on plant growth was evaluated through a controlled greenhouse experiment using the spring wheat cultivar 'Pantera.' The experiment was conducted at the Carillanca Regional Research Centre of the Instituto de Investigaciones Agropecuarias (INIA-Carillanca) Región de La Araucanía, Chile (38.6951° S, 72.4179° W). The greenhouse maintained an average daytime temperature of 22 ± 2°C, nighttime temperature of 15 ± 2°C, and relative humidity of 65 ± 5 % throughout the experiment. A 16-hour photoperiod was provided using natural sunlight supplemented with LED lamps, delivering 450 ± 50 µmol m^{-2} s^{-1} photosynthetically active radiation (PAR) to ensure uniform light exposure. The volcanic soil previously described (see Section 2.2) was used for this trial. The soil was air-dried, ground to pass through a 5 mm sieve, and thoroughly mixed.

The wheat seeds were surface sterilized by immersing them in 2 % (v/v) sodium hypochlorite for 15 minutes, followed by sowing in 7-liter plastic pots filled with soil and lined with polyethylene (dimensions: 20 × 20 × 25 cm). After germination, the seedlings were thinned to maintain four plants per pot. Four treatments were established: a control without fertilization (CT), oat hull biochar alone (OHB), conventional fertilization (CF), and the Biochar-based Controlled-Release Fertilizer with Ammonium Phosphate (BAPF). he CF treatment consisted of equivalent doses of 200 kg N ha^{-1} , 90 kg P_2O_5 ha^{-1} , 120 kg K_2O ha^{-1} using urea for N, triple superphosphate for P, and potassium-magnesium sulfate (K-Mag), respectively. All the fertilizers were applied at the plant establishment. To ensure that both the CF and BAPF treatments received identical amounts of nutrients, the BAPF was supplemented using the same inorganic fertilizers as in CF. Since BAPF contains about 3 % P, the remaining P needed to match the 90 kg P_2O_5 ha^{-1} applied in CF was provided using triple superphosphate. This approach guaranteed that the CF and BAPF treatments had equivalent nutrient inputs, enabling comparisons. Prior to the harvest, visual changes induced by the treatment were documented using RGB photography facilitated by a Canon Rebel camera, (Tokyo, Japan).

The plants were harvested at Zadok growth stage 9.1, approximately seven months after planting. Grains were manually separated, and the shoots were washed thoroughly with Milli-Q water. The washed shoots were then oven-dried at 70 °C until a constant weight was achieved, which took 48 hours. Once dried, the samples were ground into a fine powder for further analysis.

Total nitrogen (N) concentration was determined using the Dumas combustion method with a Velp Dumas-701 analyzer. For phosphorus (P) analysis, the samples were ashed at 550 °C and digested with a mixture of distilled water (H_2O), hydrochloric acid (HCl), and nitric acid (HNO_3). The phosphorus concentration in each extract was then quantified using spectrophotometry with the vanadate-molybdate method (Hanson, 1950). N and P uptake was calculated by multiplying their concentrations with the biomass of shoots, roots, or grains.

The N and P apparent recovery (AR) was calculated as follows:

$$AR(\%) = ((E_N - E_0)/F_N) \times 100 \quad (3)$$

Where E_N is the total nutrient extraction with fertilization, E_0 is the average nutrient extraction without fertilization (control, CT), and F_N is the amount of nutrient applied as fertilizer (Syers et al., 2008).

3. Experimental design and statistical analysis

For Experiment 2, a randomized design was employed with three replicates per treatment at each sampling time. Destructive sampling was conducted at 0, 1, 3, 7, 15, 30, and 60 days ($n = 72$). One-way ANOVA was performed for each time point, and Tukey's post hoc test was conducted when significant differences were found ($p < 0.05$). Statistical analyses were conducted using Infostat software (version 2008), with a significance level of $p < 0.05$.

A completely randomized design was used for the greenhouse pot trial (Experiment 3) with four treatments and three replicates ($n = 12$). ANOVA was conducted to assess differences among treatments, with prior testing of residual normality and homogeneity of variances using Shapiro-Wilk and Levene's tests, respectively. When significant differences were observed, Tukey's test was applied for multiple comparisons ($p \leq 0.05$). All statistical analyses were performed using Infostat software (version 2020e), maintaining a significance level of $p \leq 0.05$.

4. Results

Scanning electron microscopy (SEM) and energy-dispersive X-ray spectroscopy (EDX) analyses revealed distinct morphological differences between OHB and BAPF (Figs. 1 and 2). The SEM analysis showed that OHB possessed a highly porous and fibrous structure (Fig. 1b and c), whereas BAPF displayed a more compact and uniform surface (Fig. 2b and c).

The particle size distribution highlighted structural differences between both materials (Figs. 1g and 2g). BAPF exhibited a broader particle size distribution with a greater proportion of fine particles than OHB. Specifically, BAPF showed a decrease in cumulative volume percentage (Cum Q3 %) from 99 % at 3000 µm to nearly zero at smaller particle sizes, indicating the presence of fine particles (Fig. 2g). In contrast, OHB maintained a Cum Q3 % of almost 100 % down to approximately 575 µm, suggesting a dominance of larger particles with minimal fine material (Fig. 1g).

Thermogravimetric analysis (TGA) revealed that BAPF retained 88 % more moisture and had 1.8 times greater volatile matter content than OHB. This suggests that the impregnation process significantly enhances the retention of volatile compounds in BAPF (see Fig. 2i). In contrast, OHB exhibited a 76 % higher fixed carbon content (see Fig. 1i), while both materials had similar ash content, with OHB at 9.08 % and BAPF at 7.90 %.

Fourier-transform infrared (FTIR) the confirmed chemical changes due to impregnation (Fig. 1h and h). In OHB, peaks at 3400 cm^{-1} indicated O-H stretching vibrations, while peaks around 2920 cm^{-1} suggested C-H stretching vibrations of aliphatic chains. In BAPF, a reduction in these peak intensities pointed to nutrient interactions with biochar functional groups (Fig. 2i). New peaks at 1640 cm^{-1} (C═O stretching) and 1100 cm^{-1} (P–O–C stretching) confirmed the integration of N- and P-containing compounds.

Chemical composition analysis also revealed differences between OHB and BAPF, confirming the nutrient incorporation during the impregnation (Figs. 1d and 2d). Carbon content decreased from 89 % in OHB to 52.4 % in BAPF, while oxygen content increased from 6.74 % to 17.32 %, indicating the introduction of oxygenated functional groups. Nitrogen content in BAPF increased substantially, from 1.1 % to 21.4 % (Dumas combustion) and from 1.4 % to 28.3 % (Kjeldahl), confirming effective N incorporation (Fig. 2h). P content increased from 2.1 g kg^{-1} in OHB to 3.3 g kg^{-1} in BAPF, indicating P incorporation, while potassium content rose from 4.8 g kg^{-1} to 6.7 g kg^{-1}. Conversely, calcium and magnesium contents decreased from 1.0 g kg^{-1} and 1.3 g kg^{-1} in OHB to 0.4 g kg^{-1} and 0.6 g kg^{-1} in BAPF, respectively.

Therefore, physicochemical tests confirmed the N and P impregnation into OHB; however, evaluating its effect on nutrient dynamics becomes critical to ensure a controlled release of nutrients in the soil (Experiment 2).

The dynamics of soil N and P revealed distinct release patterns when comparing conventional fertilization (CF) and BAPF (Fig. 3). CF exhibited an initial rise in NH_4^+-N concentration on day 1, approximately 4.5 times greater than in the control treatment (CT). However, by day 3, this concentration decreased by about 77 % (Fig. 3c). After day 7, NH_4^+-N concentration gradually declined, reaching its lowest concentration by day 60. In contrast, NO_3^--N content in CF steadily increased from day 3 onward, reaching 28 mg kg^{-1} by day 60.

In the CF treatment, the concentration of NO_3^--N decreased by 26 % on day 3 compared to the CT treatment. An increase followed this in NO_3^--N levels on day 7, which reached 5.6 times higher than on day 3 and continued to rise until day 60 (Fig. 3d)

The BAPF have a more controlled and sustained N release than CF (Fig. 3d). The peak NH_4^+-N concentration for BAPF occurred on day 7, higher than in the unfertilized treatments (OHB and CT) but approximately 20 % lower than in CF (Fig. 3c). The NH_4^+-N concentration in BAPF gradually decreased, reaching 12.7 mg kg^{-1} by day 60. In contrast, NO_3^--N content in BAPF increased throughout the incubation period, showing a 4.2-fold increase by day 60 compared to day 1 (Fig. 3d). Total inorganic nitrogen (N_{total}) indicated that BAPF outperformed CF during the later stages of incubation, with BAPF having 6 % more N_{total} than CF by day 30 and 3 % more by day 60 (Fig. 3a).

Minimal release of NH_4^+-N and NO_3^--N was observed in the unfertilized treatments (OHB and CT). The OHB treatment displayed a slight increase in NH_4^+-N on day 3 before decreasing to minimal levels by day 30, while NO_3^--N concentrations gradually increased from 69 mg kg^{-1} on day 1–151 mg kg^{-1} by day 60. The CT treatment followed a similar trend, with slight fluctuations in NH_4^+-N and a gradual increase in NO_3^--N levels (Figs. 3b, 3c and 3d).

BAPF consistently increased P concentrations by approximately 15–25 % for soil P dynamics compared to CF, OHB, and CT treatments. The highest increase was observed on day 15, where BAPF resulted in a 25 % higher P concentration than CF and CT and a 10–18 % improvement compared to OHB (Fig. 3e).

Differences in ammonification and nitrification rates were also observed among treatments (Fig. 3g). The unfertilized treatments (CT and OHB) showed higher ammonification rates than CF and BAPF. Specifically, the CT treatment had ammonification rates approximately 3.9 and 6.4 times higher than CF and BAPF. A similar trend was observed in the OHB treatment, with net ammonification rates 2.7 and 4.4 times greater than in CF and BAPF, respectively. Nitrification rates were higher in fertilizer treatments. The BAPF had nitrification rates that were 2.6 times greater than those in the CT and OHB treatments, while CF had rates approximately 2.3 times greater than in unfertilized treatments (Fig. 3g).

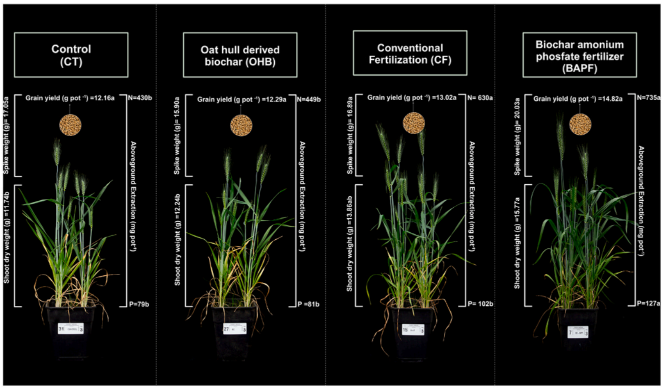

Fig. 4. Effect of the addition of oat hull-derived biochar (OHB), conventional fertilization (CF), and biochar-based controlled-release fertilizer (BAPF) on shoot dry weight, spike weight, N and P nutrient uptake, and grain yield of spring wheat (*Triticum aestivum* L. cv. Pantera), compared to the control (CT). Photos were taken during the Z6.0 growth stage.

A decrease in soil pH was observed in N-fertilized treatments compared to unfertilized ones (Fig. 3f). Specifically, the pH dropped by 0.48 units in N-fertilized soils, while reductions of approximately 0.13 units were observed in the OHB and CT treatments.

The interaction of BAPF in the soil-plant continuum was evaluated under controlled conditions (experiment 3). The application of BAPF resulted in a 34 % and 14 % increase in shoot biomass production compared to the CT and CF, respectively. Consequently, the total aboveground biomass in the BAPF treatment was 24 % higher than CT and 16 % higher than CF (Fig. 4).

The unfertilized treatments had similar N and P concentrations and uptake (Table 2). The average grain N concentration in unfertilized treatments was about 2.4 %, resulting in a total aboveground N uptake of 360 and 424 mg for CT and OHB, respectively. The CF treatment increased grain N concentration by approximately 38 % compared to CT, with P concentration being approximately 28 % higher (Table 2). Total aboveground N and P uptakes in CF were 58 % and 39 % higher than in CT, respectively. However, BAPF treatment surpassed CF in terms of N and P uptake. Although the grain N concentration under BAPF was 3.14 % (similar to CF), it developed higher aboveground biomass; hence, N uptake under BAPF was about 12 % higher than CF, resulting in a 19 % increase over CF (Fig. 4 and Table 2).

The apparent N and P recovery (ARN and ARP, respectively) also varied across treatments (Table 2). Plants treated with BAPF exhibited the highest ARN at 55.0 %, outperforming CF (ARN of 36.5 %). Differences between fertilizers were even more pronounced for P recovery, with BAPF achieving ARP values 1.1 times higher than those observed for CF (Table 2).

5. Discussion

The study presents a novel method for synthesizing a nutrient-enriched biochar-based controlled-release fertilizer. It evaluates its effectiveness from synthesis to its impacts on soil nutrient dynamics, plant growth, and yield. Several physicochemical analyses confirm that nutrients were effectively integrated into the Bc, making BAPF a promising approach for improving nutrient recovery and boosting agricultural productivity.

Scanning Electron Microscopy (SEM) analysis revealed structural changes from the impregnation (Figs. 2 and 3). The OHB exhibited a morphology typical of lignocellulosic-derived materials (González et al., 2017). It displayed porosity and surface area of 3.24 nm and 0.16 cm^2, respectively, which are associated with high adsorption capacity, indicating suitability for use as a soil amendment in productive agricultural soils and degraded areas (Curaqueo et al., 2014; Meier et al., 2017). In contrast, BAPF presented a more compact surface structure, reflecting altered pore and surface characteristics due to nutrient permeation into the Bc matrix (Fig. 2b and c).

Particle Size Analysis (PDA) provided quantitative confirmation of these structural changes, revealing a broader and finer particle size distribution in BAPF compared to OHB (Figs. 1g and 2g). Previous studies have indicated that nutrient impregnation alters the Bc's physical properties, including particle size, and improves functionality (Langella et al., 2024; Rubangakene et al., 2023). Smaller Bc particles are linked to an increased cation exchange capacity (CEC), which enhances the biochar's ability to retain and gradually release nutrients, thereby improving nutrient availability for plant uptake (Dimin et al., 2014), which is related to the effect of BAPF promoting plant growth (experiment 2, see above).

Fourier-transform infrared (FTIR) spectroscopy provided further evidence of successful impregnation by revealing changes in functional groups associated with nutrient bonding. Specifically, the reduction in peak intensities at 3400 and 2920 cm^{-1} (associated with O–H and C–H stretching vibrations, respectively) indicated interactions between the Bc's functional groups and the impregnated nutrients (González et al., 2017). The presence of new peaks around 1600 cm^{-1} may indicate the formation of amide groups,

Table 2
Concentrations and extractions of nitrogen (N) and phosphorus (P) in tillers, grains, and roots, along with the apparent nutrient recovery in the wheat cultivar 'Pantera', evaluated under four soil treatments: CT (control, no amendment); OHB (oat hull biochar applied at the same weight-for-weight dose as BAPF); CF (conventional fertilization equivalent to 200 kg N ha^{-1}); and BAPF (biochar ammonium phosphate fertilizer). According to Tukey's multiple comparison tests ($p < 0.05$), different letters in the row indicate significant differences among treatments.

	CT	OHB	CF	BAPF
N concentration (mg g^{-1})				
Shoots	0.36 ± 0.02^{b}	0.40 ± 0.01^{b}	0.77 ± 0.07^{a}	0.69 ± 0.07^{a}
Grains	2.28 ± 0.06^{b}	2.52 ± 0.09^{b}	3.14 ± 0.02^{a}	3.14 ± 0.07^{a}
Roots	0.99 ± 0.05^{c}	1.21 ± 0.04^{b}	1.34 ± 0.08^{ab}	1.47 ± 0.03^{a}
N extraction (mg pot^{-1})				
Shoots	42.0 ± 2.6^{b}	49.1 ± 3.3^{b}	100.1 ± 3.5^{a}	107.8 ± 11.1^{a}
Grains	276.9 ± 10.8^{b}	308.84 ± 25.6^{b}	409.20 ± 22.6^{a}	465.2 ± 9.1^{a}
Roots	40.7 ± 3.8^{b}	32.6 ± 2.9^{b}	60.1 ± 5.9^{a}	65.9 ± 3.4^{a}
N apparent recovery (%)	——	——	**36.5 ± 5.9 %^{b}**	**55.0 % ± 2.8 %^{a}**
P concentration (mg g^{-1})				
Shoots	0.02 ± 0.002^{b}	0.03 ± 0.004^{b}	0.05 ± 0.003^{a}	0.05 ± 0.005^{a}
Grains	0.45 ± 0.01^{b}	$0.49 \pm 0{,}01^{b}$	0.57 ± 0.02^{a}	0.60 ± 0.01^{a}
Roots	0.11 ± 0.02^{a}	$0.10 \pm 0{,}01^{a}$	0.11 ± 0.01^{a}	0.13 ± 0.01^{a}
P extraction (mg pot^{-1})				
Shoots	2.6 ± 0.3^{b}	3.7 ± 0.5^{b}	6.9 ± 0.5^{a}	7.9 ± 0.6^{a}
Grains	54.1 ± 2.1^{c}	59.7 ± 4.2^{bc}	74.0 ± 5.9^{ab}	88.9 ± 1.9^{a}
Roots	5.0 ± 0.5^{a}	2.35 ± 0.1^{b}	5.1 ± 0.6^{a}	5.6 ± 0.4^{a}
P apparent recovery (%)	——	——	**8.9 % ± 3.6 %^{a}**	**18.5 % ± 1.0 %^{a}**

potentially resulting from the reactions between urea and the Bc matrix (González et al., 2017). Additional bands at 1450 and 1150 cm^{-1} were linked to C–N axial deformation (Barbosa et al., 2022), and the peaks at 1200–1100 cm^{-1} were attributed to the chelation of phosphate groups during adsorption (El Sharkawi et al., 2018; Shakoor et al., 2021).

The chemical characterization also confirmed differences in elemental composition between OHB and BAPF (Figs. 1d and 2d). Oats' high potassium (K) content is due to their nutrient distribution, as they retain over 90 % of absorbed potassium in the straw (Fulton and Findlay, 1965). Other elements, such as calcium (Ca) and magnesium (Mg), were lower in BAPF than OHB, potentially due to dilution effects resulting from substantial N and P additions or interactions during the impregnation process that affected biochar's mineral composition.

Finally, the thermogravimetric Analysis (TGA) also provided essential insights into the stability and retention of nutrients within BAPF. The TGA results showed that BAPF retained more moisture and exhibited a higher volatile matter content than OHB. This suggests that the nutrients were effectively bound to the biochar matrix, altering its thermal stability (Pandian et al., 2024). The increased retention of volatile compounds and the shifts in decomposition temperatures further indicate the successful integration of nutrients into the Bc structure (Albalasmeh et al., 2024).

The functional-release properties of BAPF were evident during the eight-week incubation study. Unlike conventional fertilizers (CF), which exhibited irregular NH_4^+-N release patterns, especially during the initial incubation days (Fig. 3), BAPF demonstrated a gradual and sustained release of both NH_4^+-N and NO_3^--N. This controlled-release behavior can be attributed to the adsorption and gradual desorption of NH_4^+ ions within the porous structure of biochar (Yao et al., 2012). The high surface area, porosity, and functional groups in biochar help retain NH_4^+-N, thus slowing its release into the soil solution compared to CF, which has been described by previous reports (Liu et al., 2018; Woolf et al., 2010).

The steady increase in NO_3^--N concentrations in the BAPF treatment indicates enhanced nitrification over time, likely due to the controlled release of NH_4^+-N, which provided a substrate for nitrifying bacteria (Gao et al., 2019). Similar results were reported by Nguyen et al. (2017), who found that Bc improved soil aeration and moisture, enhancing nitrifier activity. This effect was more pronounced when Bc was combined with ammonium-based fertilizers, which offered an increased substrate for nitrification. Additionally, Mandal et al. (2016) reported a 6.5 % increase in total N content with biochar-based fertilizers after 8 weeks of incubation, while Nguyen et al. (2017) observed that biochar-amended soils had 5–8 % higher total nitrogen content compared to control and conventional fertilizer treatments after two months. Furthermore, Gao et al. (2019) reported a 7.2 % increase in total N content with BC-based fertilizers after 60 days, suggesting a more consistent nutrient supply.

Differences in ammonification and nitrification rates were observed, highlighting the impact of N sources on soil nutrient dynamics (Fig. 3g). Treatments without added N (CT and OHB) exhibited higher ammonification rates, likely due to the absence of external N inputs, prompting microorganisms to increase organic matter mineralization to meet their N demands. These observations are consistent with previous findings that soils lacking N fertilization rely more heavily on the mineralization of organic matter for nutrient supply (Clough and Condron, 2010; Nelson et al., 2011; Wang et al., 2022, 2018; Zhang et al., 2015). The study was conducted on Andisol, a soil known for its high organic matter content (Table 1), which may explain the high mineralization rates observed (Matus et al., 2014). The interaction between organic compounds and allophane minerals typical of Andisols likely promoted these mineralization dynamics (Curaqueo et al., 2021; Matus et al., 2014). On the contrary, treatments with added N (CF and BAPF) exhibited higher nitrification rates compared to unfertilized ones (CT and OHB), suggesting that initial N addition stimulates nitrification activity (Fig. 3g). Elevated NH_4^+ concentrations from fertilization provide more substrate for nitrifying bacteria, enhancing NO_3^- formation. This is consistent with findings that inorganic N fertilization, particularly ammonium-based fertilizers, promotes nitrification in acidic soils (Li et al., 2018b). Furthermore, biochar-based fertilizers improved soil properties such as porosity, oxygen availability, and water-holding capacity, fostering an environment conducive to nitrifying bacteria (Gul et al., 2015; Verheijen et al., 2010).

The higher available P concentrations observed in BAPF treatments likely resulted from phosphate adsorption onto biochar surfaces and subsequent gradual desorption (Cui et al., 2011; Glaser and Lehr, 2019; Nelson et al., 2011; Wang et al., 2012). Functional groups in biochar, such as hydroxyl and carboxyl, may temporarily bind phosphate, acting as a slow-release source of P (Nelson et al., 2011). This mechanism helps reduce P fixation, particularly in volcanic soils with high phosphorus sorption capacity, thereby enhancing P recovery (Curaqueo et al., 2013; Seguel et al., 2017). These findings align with the BAPF characterization from Experiment 1, where structural and physicochemical analyses confirmed modifications in BAPF that contribute to its controlled nutrient release. Additionally, thermogravimetric analysis demonstrated improved moisture retention, explaining how BAPF influences nutrient solubilization based on soil moisture levels. This framework clarifies why BAPF achieved 6 % higher N- controlled release and 20 % greater phosphorus availability than conventional fertilizers by day 60, highlighting the link between biochar properties and its ability to regulate nutrient availability over time. Beyond nutrient controlled release, BAPF also influenced soil pH dynamics, particularly through its interaction with nitrification processes. During nitrification, ammonium (NH_4^+) oxidation to nitrate (NO_3^-) releases hydrogen ions (H^+), leading to acidification (Ni et al., 2023). In BAPF-amended soils, increased nitrification activity resulted in slight acidification (Fig. 3f), correlating with quantified nitrification rates (Fig. 3g). However, the biochar component in BAPF likely mitigated extreme pH declines through its alkaline functional groups (e.g., phenols) and carbonate content, buffering pH fluctuations despite similar nitrification intensity as conventional fertilizers (Hina et al., 2010; Zhang et al., 2016).

Maintaining soil pH within the optimal range (5.5–6.5) is particularly crucial for P solubility in Andisols (Curaqueo et al., 2021). Conversely, unfertilized treatments showed minimal acidification, consistent with natural soil acidification processes (Borie and Rubio, 2003). The ability of BAPF to buffer soil pH suggests it can contribute to more favorable conditions for plant growth, reducing the risks associated with soil acidification (Silber et al., 2010).

BAPF demonstrated significant agronomic effectiveness, improving plant growth, nutrient uptake, and grain yield more efficiently than conventional fertilizers (CF) and unfertilized controls (Fig. 4). This suggests a synergistic interaction between biochar and inorganic fertilizers, optimizing nutrient availability and uptake.

Nutrient dynamics analysis (Table 2) highlights BAPF's superior performance. BAPF-treated plants showed significantly higher root nitrogen concentration ($p < 0.05$), indicating better nutrient acquisition and rhizosphere interactions. For phosphorus, BAPF enhanced grain P extraction significantly ($p < 0.05$) compared to CF and unfertilized treatments, which is important in high P-fixing Andisols.

BAPF-treated plants also had higher nitrogen and phosphorus uptake, with apparent N recovery (ARN) at 55.0 %, a 50.7 % increase over CF (36.5 %, $p < 0.05$). Phosphorus recovery (ARP) also doubled (18.5 % vs. 8.9 %), although variability in CF reduced statistical significance. These gains are likely linked to higher yields, as nutrient release better matched the crops' physiological needs throughout their growth stages.

Prior studies have shown improved nitrogen recovery with biochar-urea mixtures across various crops, reporting ARN increases between 10 % and 60 % compared to conventional fertilizers (Banik et al., 2023; Cao et al., 2021; Cui et al., 2022; Liao et al., 2020; Ning et al., 2022). Specifically, (Shi et al., 2022) found a net ARN increase of 10–20 % in wheat, while (Ghorbani et al., 2022) reported a 14 % increase when biochar was combined with urea. Few studies, however, have evaluated the efficiency of biochar as a phosphorus carrier until full plant maturity. (Pogorzelski et al., 2020) found an increase of 10–20 % in P recovery efficiency using biochar enriched with triple superphosphate, which closely matches our study's results.

Notably, the effectiveness of BAPF was demonstrated in an Andisol (Barros Arana Series), a volcanic soil with exceptionally high P-fixing potential (>75 %) due to its allophanic mineralogy and strong ligand exchange mechanisms (Borie and Rubio, 2003). The observed improvement in P availability under such conditions suggests that BAPF could also be effective in soils with lower sorption capacities.

While this study was conducted in a high P-fixing soil, BAPF performance may vary depending on soil physicochemical properties. In calcareous soils (pH >7.5), where P availability is primarily constrained by Ca-phosphate precipitation rather than Al/Fe sorption (Hui et al., 2019; Luo et al., 2023), BAPF might exhibit altered release kinetics but could still enhance P availability through localized acidification at the biochar-soil interface (Majeed et al., 2015; Narayanasamy et al., 2023). Conversely, in sandy soils with low cation exchange capacity and minimal P fixation, BAPF could potentially reduce P leaching while maintaining nutrient availability (El Sharkawi et al., 2018). However, further investigations are needed to assess BAPF performance across different soil types to determine its effectiveness under varying pedological conditions and optimize formulations for distinct agricultural systems.

Finally, the superior performance of BAPF over CF can be attributed to the synergistic effect between biochar and inorganic fertilizers. Biochar enhances soil cation exchange capacity, reduces nutrient leaching, and ensures a steady nutrient supply for plants. It also improves soil aeration and water retention and supports microbial activity, creating favorable conditions for root development and nutrient uptake. By fostering microbial activity, biochar promotes nutrient cycling and makes nutrients more accessible for plant uptake. This combination improves nutrient availability and consequently enhances plant growth and yield. Incorporating biochar with inorganic fertilizers facilitates a controlled, gradual nutrient release that aligns with plant requirements, reducing nutrient losses and improving overall efficiency (Gao et al., 2019; He et al., 2022; Shi et al., 2022). Despite equivalent nutrient doses, BAPF's superior performance compared to CF indicates that integrating biochar enhances fertilizer effectiveness by improving nutrient retention, soil structure, and microbial activity. BAPF's controlled-release properties improved nutrient retention compared to conventional fertilization, reducing potential N and P losses over time. BAPF's controlled-release properties improved nutrient retention compared to conventional fertilization, reducing potential N and P losses over time. In volcanic Andisols, where P fixation is high and N leaching remains problematic, BAPF facilitated a more gradual nutrient release, enhancing availability while minimizing residual losses. The observed nitrification patterns suggest a more synchronized conversion of N into plant-available forms, reducing susceptibility to leaching. These findings highlight BAPF's potential as a sustainable strategy to enhance soil fertility, plant growth, and agricultural productivity.

6. Conclusions

This study developed a biochar-based controlled-release fertilizer (BAPF) by impregnating oat hull biochar with urea and diammonium phosphate. Physicochemical characterization confirmed successful nutrient integration, with carbon content decreasing by nearly 40 %, nitrogen increasing twentyfold, and notable structural modifications observed in FTIR spectra and particle size distribution.

Soil incubation experiments demonstrated that BAPF sustained higher nutrient availability, maintaining 6 % higher total nitrogen and over 20 % more available phosphorus than conventional fertilization by day 60. Nitrification rates were twice as high as in unfertilized treatments, suggesting a more efficient nitrogen conversion process that reduces susceptibility to losses.

In greenhouse trials, BAPF-treated wheat exhibited improved growth, nutrient uptake, and grain yield. Total biomass and grain yield increased by approximately 15 % compared to conventional fertilization. Apparent nitrogen recovery increased by over 50 %, while phosphorus recovery more than doubled, reinforcing BAPF's potential to mitigate phosphorus fixation in volcanic soils. BAPF also increased nutrient uptake, with nitrogen uptake improving by 16 % and phosphorus uptake by 30 % compared to traditional fertilizer, highlighting its efficiency in nutrient delivery.

These improvements can be attributed to the combined effects of biochar's nutrient retention properties and the controlled-release mechanism of the nutrients. Overall, BAPF shows potential as a sustainable fertilization strategy by enhancing nutrient use efficiency, reducing nutrient losses, and supporting crop productivity. This approach could contribute to more sustainable agricultural practices by reducing fertilizer inputs and minimizing environmental impacts.

Future research should evaluate the effectiveness of BAPF under field conditions over multiple growing seasons. Long-term field studies must assess BAPF's impact on soil quality, nutrient dynamics, and crop productivity under varying environmental conditions and agricultural management practices. Additionally, such studies would provide valuable insights into the economic viability and practical application of biochar-based controlled-release fertilizers in sustainable agriculture.

CRediT authorship contribution statement

María-Eugenia González: Methodology, Investigation. **Naser Khan**: Methodology, Investigation. Juan Hirzel:Investigation. **Sigrid Muñoz**: Methodology, Investigation. **Gabrijel Ondrasekh**: Methodology, Investigation, Data curation. **Sebastián Meier**: Writing – original draft, Validation, Methodology, Investigation. **Pedro M. de Souza Campos**: Writing – original draft, Methodology, Investigation, Formal analysis. **Alex Seguel**: Writing – review & editing, Writing – original draft, Validation, Supervision, Project administration, Investigation, Funding acquisition. **Rubén Palma**: Methodology, Investigation, Formal analysis, Data curation. **Natalia Rojas**: Methodology, Investigation.

Declaration of Competing Interest

The authors declare that they have no known competing financial interests or personal relationships that could have appeared to influence the work reported in this paper.

Acknowledgments

The National Agency for Research and Development ANID-Chile funded this through the FONDECYT project, 1211387 (A. Seguel) and 1220190 (S. Meier).

Data availability

Data will be made available on request.

References

Albalasmeh, A.A., Quzaih, M.Z., Gharaibeh, M.A., Rusan, M., Mohawesh, O.E., Rababah, S.R., Alqudah, A., Alghamdi, A.G., Naserin, A., 2024. Significance of pyrolytic temperature, application rate and incubation period of biochar in improving hydro-physical properties of calcareous sandy loam soil. Sci. Rep. 14. https://doi.org/10.1038/s41598-024-57755-y.

Anas, M., Liao, F., Verma, K.K., Sarwar, M.A., Mahmood, A., Chen, Z.L., Li, Q., Zeng, X.P., Liu, Y., Li, Y.R., 2020. Fate of nitrogen in agriculture and environment: agronomic, eco-physiological and molecular approaches to improve nitrogen use efficiency. Biol. Res. https://doi.org/10.1186/s40659-020-00312-4.

Atkinson, C.J., 2018. How good is the evidence that soil-applied biochar improves water-holding capacity? Soil Use Manag. 34, 177–186. https://doi.org/10.1111/sum.12413.

Banik, C., Bakshi, S., Laird, D.A., Smith, R.G., Brown, R.C., 2023. Impact of biochar-based slow-release N-fertilizers on maize growth and nitrogen recovery efficiency. J. Environ. Qual. 52, 630–640. https://doi.org/10.1002/jeq2.20468.

Barbosa, C.F., Correa, D.A., Carneiro, J.S. da S., Melo, L.C.A., 2022. Biochar phosphate fertilizer loaded with urea preserves available nitrogen longer than conventional urea. Sustainability 14. https://doi.org/10.3390/su14020686.

Borie, F., Rubio, R., 2003. Total and organic phosphorus in Chilean volcanic soils. Gayana. Botánica 60, 69–78. https://doi.org/10.4067/S0717-66432003000100011.

Calabi-Floody, M., Medina, J., Rumpel, C., Condron, L.M., Hernandez, M., Dumont, M., Mora, M. de la L., 2018. Smart Fertilizers as a Strategy for Sustainable Agriculture. Advances in Agronomy. Academic Press Inc., pp. 119–157. https://doi.org/10.1016/bs.agron.2017.10.003

Cao, X., Yuan, L., Liu, X., Zhu, L., Zhu, C., Kong, Y., Wu, L., Tian, C., Lu, R., Zhang, J., Yu, Y., Jin, Q., 2021. Benefits of controlled-release/stable fertilizers plus biochar for rice grain yield and nitrogen utilization under alternating wet and dry irrigation. Eur. J. Agron. 129. https://doi.org/10.1016/j.eja.2021.126338.

Carneiro, J.S.D.S., Lustosa Filho, J.F., Nardis, B.O., Ribeiro-Soares, J., Zinn, Y.L., Melo, L.C.A., 2018. Carbon stability of engineered biochar-based phosphate fertilizers. ACS Sustain Chem. Eng. 6, 14203–14212. https://doi.org/10.1021/acssuschemeng.8b02841.

Ciampitti, I.A., Vyn, T.J., 2014. Understanding global and historical nutrient use efficiencies for closing maize yield gaps. Agron. J. 106, 2107–2117. https://doi.org/10.2134/agronj14.0025.

CIREN, 2002. Descripciones de Suelos y Materiales y Simbolos. Estudio Agrologico IX Región. Publicación CIREN N° 122. 338p.

Clough, T.J., Condron, L.M., 2010. Biochar and the Nitrogen Cycle: Introduction. J Environ Qual 39, 1218–1223. https://doi.org/Doi 10.2134/Jeq2010.0204.

Cormier, F., Foulkes, J., Hirel, B., Gouache, D., Moënne-Loccoz, Y., Le Gouis, J., 2016. Breeding for increased nitrogen-use efficiency: a review for wheat (T. aestivum L.). Plant Breed. 135, 255–278. https://doi.org/10.1111/pbr.12371.

Cui, P., Chen, Z., Ning, Q., Wei, H., Zhang, Haipeng, Lu, H., Gao, H., Zhang, Hongcheng, 2022. One-time nitrogen fertilizer application using controlled-release urea ensured the yield, nitrogen use efficiencies, and profits of winter wheat. Agronomy 12. https://doi.org/10.3390/agronomy12081792.

Cui, H.J., Wang, M.K., Fu, M.L., Ci, E., 2011. Enhancing phosphorus availability in phosphorus-fertilized zones by reducing phosphate adsorbed on ferrihydrite using rice straw-derived biochar. J. Soils Sediment. 11, 1135–1141. https://doi.org/10.1007/s11368-011-0405-9.

Curaqueo, G., González, A., Cea, M., Meier, S., Borie, F., Navia, R., 2013. Use of Biochar in volcanic soils of Southern Chile and its effect on yield parameters of Hordeum vulgare, in: 17th Conference of the Internacional Organization for Soil. Medellín, p. 277.

Curaqueo, G., Meier, S., Khan, N., Cea, M., Navia, R., 2014. Use of biochar on two volcanic soils: effects on soil properties and barley yield. J. Soil Sci. Plant Nutr. 14.

Curaqueo, G., Roldán, A., Mutis, A., Panichini, M., Pérez-San Martín, A., Meier, S., Mella, R., 2021. Effects of biochar amendment on wheat production, mycorrhizal status, soil microbial community, and properties of an Andisol in Southern Chile. Field Crops Res. 273. https://doi.org/10.1016/j.fcr.2021.108306.

Dimin, M.F., Se, S.M., Shaaban, A., Hashim, M.M., 2014. Urea impregnated biochar to minimize nutrients loss in paddy soils. Int. J. Automot. Mech. Eng. 10, 2016–2024. https://doi.org/10.15282/ijame.10.2014.18.0169.

El Sharkawi, H.M., Tojo, S., Chosa, T., Malhat, F.M., Youssef, A.M., 2018. Biochar-ammonium phosphate as an uncoated-slow release fertilizer in sandy soil. Biomass Bioenergy 117, 154–160. https://doi.org/10.1016/j.biombioe.2018.07.007.

Fulton, J., Findlay, 1965. Influence of Soil Moisture and Ambient Temperature on Nutrient Percentage of Oat Tissue 75–82.

Galloway, J.N., Winiwarter, W., Leip, A., Leach, A.M., Bleeker, A., Erisman, J.W., 2014. Nitrogen footprints: past, present and future. Environ. Res. Lett. 9. https://doi.org/10.1088/1748-9326/9/11/115003.

Gao, S., DeLuca, T.H., Cleveland, C.C., 2019. Biochar additions alter phosphorus and nitrogen availability in agricultural ecosystems: a meta-analysis. Sci. Total Environ. https://doi.org/10.1016/j.scitotenv.2018.11.124.

Gao, Y., Fang, Z., Van Zwieten, L., Bolan, N., Dong, D., Quin, B.F., Meng, J., Li, F., Wu, F., Wang, H., Chen, W., 2022. A critical review of biochar-based nitrogen fertilizers and their effects on crop production and the environment. Biochar. https://doi.org/10.1007/s42773-022-00160-3.

Ghorbani, M., Konvalina, P., Neugschwandtner, R.W., Kopecký, M., Amirahmadi, E., Bucur, D., Walkiewicz, A., 2022. Interaction of biochar with chemical, green and biological nitrogen fertilizers on nitrogen use efficiency indices. Agronomy 12. https://doi.org/10.3390/agronomy12092106.

Glaser, B., Lehr, V.I., 2019. Biochar effects on phosphorus availability in agricultural soils: a meta-analysis. Sci. Rep. 9. https://doi.org/10.1038/s41598-019-45693-z.

González, M.E., Cea, M., Medina, J., González, A., Diez, M.C., Cartes, P., Monreal, C., Navia, R., 2015. Evaluation of biodegradable polymers as encapsulating agents for the development of a urea controlled-release fertilizer using biochar as support material. Sci. Total Environ. 505, 446–453.

González, M.E., Cea, M., Reyes, D., Romero-Hermoso, L., Hidalgo, P., Meier, S., Benito, N., Navia, R., 2017. Functionalization of biochar derived from lignocellulosic biomass using microwave technology for catalytic application in biodiesel production. Energy Convers. Manag 137. https://doi.org/10.1016/j.enconman.2017.01.063.

Güereña, D., Lehmann, J., Hanley, K., Enders, A., Hyland, C., Riha, S., 2013. Nitrogen dynamics following field application of biochar in a temperate North American maize-based production system. Plant Soil 365, 239–254. https://doi.org/10.1007/s11104-012-1383-4.

Gul, S., Whalen, J.K., Thomas, B.W., Sachdeva, V., Deng, H., 2015. Physico-chemical properties and microbial responses in biochar-amended soils: mechanisms and future directions. Agric. Ecosyst. Environ. 206, 46–59. https://doi.org/10.1016/j.agee.2015.03.015.

Gul, S., Whalen, J.K., 2016. Biochemical cycling of nitrogen and phosphorus in biochar-amended soils. Soil Biol. Biochem. https://doi.org/10.1016/j.soilbio.2016.08.001.

Hanson, W.C., 1950. The photometric determination of phosphorus in fertilizers using the phosphovanado-molybdate complex. J. Sci. Food Agric. 1, 172–173. https://doi.org/10.1002/jsfa.2740010604.

He, Q., Li, X., Ren, Y., 2022. Analysis of the simultaneous adsorption mechanism of ammonium and phosphate on magnesium-modified biochar and the slow release effect of fertiliser. Biochar 4. https://doi.org/10.1007/s42773-022-00150-5.

Hina, K., Bishop, P., Arbestain, M.C., Calvelo-Pereira, R., Macia-Agullo, J.A., Hindmarsh, J., Hanly, J.A., Macias, F., Hedley, M.J., 2010. Producing biochars with enhanced surface activity through alkaline pretreatment of feedstocks. Aust. J. Soil Res. 48, 606–617. https://doi.org/10.1071/Sr10015.

Hui, X., Luo, L., Wang, S., Cao, H., Huang, M., Shi, M., Malhi, S.S., Wang, Z., 2019. Critical concentration of available soil phosphorus for grain yield and zinc nutrition of winter wheat in a zinc-deficient calcareous soil. Plant Soil 444, 315–330. https://doi.org/10.1007/s11104-019-04273-w.

Khalid, A., Hameed, A., Tahir, M.F., 2023. Wheat quality: a review on chemical composition, nutritional attributes, grain anatomy, types, classification, and function of seed storage proteins in bread making quality. Front. Nutr. https://doi.org/10.3389/fnut.2023.1053196.

Langella, T., Mikulijan, M., Han, L., Zouari, M., DeVallance, D.B., 2024. Modification of wood via biochar particle impregnation. Eur. J. Wood Wood Prod. 82, 773–783. https://doi.org/10.1007/s00107-023-02032-4.

Lehmann, J., Joseph, S., 2009. Biochar for Environmental Management.

Li, Y., Chapman, S.J., Nicol, G.W., Yao, H., 2018. Nitrification and nitrifiers in acidic soils. Soil Biol. Biochem. https://doi.org/10.1016/j.soilbio.2017.10.023.

Li, P., Lu, J., Wang, Y., Wang, S., Hussain, S., Ren, T., Cong, R., Li, X., 2018. Nitrogen losses, use efficiency, and productivity of early rice under controlled-release urea. Agric. Ecosyst. Environ. 251, 78–87. https://doi.org/10.1016/j.agee.2017.09.020.

Liang, Y., Cao, X., Zhao, L., Arellano, E., 2014. Biochar- and phosphate-induced immobilization of heavy metals in contaminated soil and water: implication on simultaneous remediation of contaminated soil and groundwater. Environ. Sci. Pollut. Res. 21, 4665–4674. https://doi.org/10.1007/s11356-013-2423-1.

Liao, J., Liu, X., Hu, A., Song, H., Chen, X., Zhang, Z., 2020. Effects of biochar-based controlled release nitrogen fertilizer on nitrogen-use efficiency of oilseed rape (Brassica napus L.). Sci. Rep. 10. https://doi.org/10.1038/s41598-020-67528-y.

Liu, Q., Zhang, Y., Liu, B., et al., 2018. How does biochar influence soil N cycle? A meta-analysis. Plant Soil 426, 211–225. https://doi.org/10.1007/s11104-018-3619-4.

López-Arredondo, D.L., Leyva-González, M.A., González-Morales, S.I., López-Bucio, J., Herrera-Estrella, L., 2014. Phosphate nutrition: improving low-phosphate tolerance in crops. Annu Rev. Plant Biol. 65, 95–123. https://doi.org/10.1146/annurev-arplant-050213-035949.

Luo, L., Zhang, X., Zhang, M., Wei, P., Chai, R., Wang, Y., Zhang, C., Siddique, K.H.M., 2023. Improving wheat yield and phosphorus use efficiency through the optimization of phosphorus fertilizer types based on Soil P Pool characteristics in calcareous and non-calcareous soil. Agronomy 13. https://doi.org/10.3390/agronomy13030928.

Majeed, Z., Ramli, N.K., Mansor, N., Man, Z., 2015. A comprehensive review on biodegradable polymers and their blends used in controlled-release fertilizer processes. Rev. Chem. Eng. 31, 69–95. https://doi.org/10.1515/revce-2014-0021.

Mandal, S., Thangarajan, R., Bolan, N.S., Sarkar, B., Khan, N., Ok, Y.S., Naidu, R., 2016. Biochar-induced concomitant decrease in ammonia volatilization and increase in nitrogen use efficiency by wheat. Chemosphere 142, 120–127. https://doi.org/10.1016/j.chemosphere.2015.04.086.

Martínez-Dalmau, J., Berbel, J., Ordóñez-Fernández, R., 2021. Nitrogen fertilization. A review of the risks associated with the inefficiency of its use and policy responses. Sustainability. https://doi.org/10.3390/su13105625.

Matus, F., Rumpel, C., Neculman, R., Panichini, M., Mora, M.L., 2014. Soil carbon storage and stabilisation in andic soils: a review. Catena. https://doi.org/10.1016/j.catena.2014.04.008.

Meier, S., Curaqueo, G., Khan, N., Bolan, N., Rilling, J., Vidal, C., Fernández, N., Acuña, J., González, M.E., Cornejo, P., Borie, F., 2017. Effects of biochar on copper immobilization and soil microbial communities in a metal-contaminated soil. J. Soils Sediment. 17, 1237–1250. https://doi.org/10.1007/s11368-015-1224-1.

Narayanasamy, R., Thiyagarajan, C., Pillai, M.P., Muthunalliappan, M., Subburamu, K., Subramanian, M., 2023. Nutrient release from biodegradable polymer-coated multi-nutrient fertilizer granules in calcareous soils. Arab. J. Geosci. 16. https://doi.org/10.1007/s12517-022-11136-9.

Nayak, B.K., Chatterjee, D., Paul, R., Das, S.R., Adak, T., Mandal, N., Drewer, J., Pradhan, A., Kundu, M.C., Pal, A.K., Santra, G.H., Sahoo, S., Datta, S.C., Sutton, M.A., Nayak, A.K., Pathak, H., 2025. Review of nano-clay polymer composites for controlled nitrogen release: prospects and limitations. Agric. Res. https://doi.org/10.1007/s40003-025-00848-5.

Nayak, P., Nandipamu, T.M.K., Chaturvedi, S., Dhyani, V.C., Chandra, S., 2024. Synthesis, properties, and mechanistic release-kinetics modeling of biochar-based slow-release nitrogen fertilizers and their field efficacy. J. Soil Sci. Plant Nutr. https://doi.org/10.1007/s42729-024-02052-w.

Nelson, N.O., Agudelo, S.C., Yuan, W.Q., Gan, J., 2011. Nitrogen and phosphorus availability in biochar-amended soils. Soil Sci. 176, 218–226. https://doi.org/10.1097/Ss.0b013e3182171eac.

Nguyen, T.T.N., Xu, C.Y., Tahmasbian, I., Che, R., Xu, Z., Zhou, X., Wallace, H.M., Bai, S.H., 2017. Effects of biochar on soil available inorganic nitrogen: a review and meta-analysis. Geoderma. https://doi.org/10.1016/j.geoderma.2016.11.004.

Ni, G., Leung, P.M., Daebeler, A., Guo, J., Hu, S., Cook, P., Nicol, G.W., Daims, H., Greening, C., 2023. Nitrification in acidic and alkaline environments. Essays Biochem. https://doi.org/10.1042/EBC20220194.

Ning, C., Liu, R., Kuang, X., Chen, H., Tian, J., Cai, K., 2022. Nitrogen fertilizer reduction combined with biochar application maintain the yield and nitrogen supply of rice but improve the nitrogen use efficiency. Agronomy 12. https://doi.org/10.3390/agronomy12123039.

Pandian, K., Vijayakumar, S., Mustaffa, M.R.A.F., Subramanian, P., Chitraputhirapillai, S., 2024. Biochar – A sustainable soil conditioner for improving soil health, crop production and environment under changing climate: a review. Front. Soil Sci. https://doi.org/10.3389/fsoil.2024.1376159.

Pereira, V.V., Morales, M.M., Pereira, D.H., de Rezende, F.A., de Souza Magalhães, C.A., de Lima, L.B., Marimon-Junior, B.H., Petter, F.A., 2022. Activated biochar-based organomineral fertilizer delays nitrogen release and reduces N2O emission. Sustainability 14. https://doi.org/10.3390/su141912388.

Pogorzelski, D., Filho, J.F.L., Matias, P.C., Santos, W.O., Vergütz, L., Melo, L.C.A., 2020. Biochar as composite of phosphate fertilizer: characterization and agronomic effectiveness. Sci. Total Environ. 743. https://doi.org/10.1016/j.scitotenv.2020.140604.

Rubangakene, N.O., Elwardany, A., Fujii, M., Sekiguchi, H., Shokry, H., 2023. Influence of Impregnation of sodium carbonate catalyst on physicochemical properties of biochar †. Eng. Proc. 37. https://doi.org/10.3390/ECP2023-14688.

Sadzawka, A., Carrasco, M.A., Grez, R., Mora, M., Flores, H., Neaman, A., Agropecuarias, I. de I., 2006. Métodos de análisis recomendados para los suelos de Chile. Instituto de Investigaciones Agropecuarias. 164 p., Santiago de Chile, Chile.
Saha, B.K., Rose, M.T., Wong, V.N.L., Cavagnaro, T.R., Patti, A.F., 2018. Nitrogen dynamics in soil fertilized with slow release brown coal-urea fertilizers. Sci. Rep. 8. https://doi.org/10.1038/s41598-018-32787-3.
Sandoval, M., Dörner, J., Seguel, O., Cuevas, J., Rivera, D., 2012. Métodos de análisis físico de suelos. Publ. Dep. De. Suelos Y. Recur. Nat. 5, 80.
Seguel, A., Cornejo, P., Ramos, A., Von Baer, E., Cumming, J., Borie, F., 2017. Phosphorus acquisition by three wheat cultivars contrasting in aluminium tolerance growing in an aluminium-rich volcanic soil. Crop Pasture Sci. 68, 305–316. https://doi.org/10.1071/CP16224.
Shakoor, M.B., Ye, Z.L., Chen, S., 2021. Engineered biochars for recovering phosphate and ammonium from wastewater: a review. Sci. Total Environ. https://doi.org/10.1016/j.scitotenv.2021.146240.
Shi, W., Bian, R., Li, L., Lian, W., Liu, X., Zheng, J., Cheng, K., Zhang, X., Drosos, M., Joseph, S., Pan, G., 2022. Assessing the impacts of biochar-blended urea on nitrogen use efficiency and soil retention in wheat production. GCB Bioenergy 14, 65–83. https://doi.org/10.1111/gcbb.12904.
Silber, A., Bar-Yosef, B., Levkovitch, I., Soryano, S., 2010. pH-Dependent surface properties of perlite: Effects of plant growth. Geoderma 158 (3–4), 275–281. https://doi.org/10.1016/j.geoderma.2010.05.006. ISSN 0016-7061.
Syers, J.K., Johnston, A.E., Curtin, D., 2008. Efficiency of soil and fertilizer phosphorus use. FAO Fertil. Plant Nutr. Bull. 18.
Thangarajan, R., Bolan, N.S., Tian, G., Naidu, R., Kunhikrishnan, A., 2013. Role of organic amendment application on greenhouse gas emission from soil. Sci. Total Environ. https://doi.org/10.1016/j.scitotenv.2013.01.031.
Tomczyk, A., Sokołowska, Z., Boguta, P., 2020. Biochar physicochemical properties: pyrolysis temperature and feedstock kind effects. Rev. Environ. Sci. Biotechnol. https://doi.org/10.1007/s11157-020-09523-3.
Vandamme, E., Wissuwa, M., Rose, T., Dieng, I., Drame, K.N., Fofana, M., Senthilkumar, K., Venuprasad, R., Jallow, D., Segda, Z., Suriyagoda, L., Sirisena, D., Kato, Y., Saito, K., 2016. Genotypic variation in grain P loading across diverse rice growing environments and implications for field P balances. Front. Plant Sci. 7. https://doi.org/10.3389/fpls.2016.01435.
Verheijen, F., Jeffery, S., Bastos, A.C., Van der Velde, M., Diafas, I., 2010. Biochar application to soils. A critical scientific review of effects on soil properties, processes and functions, JRC Scientific and Technical Reports. EUR 24099 EN. Off. Off. Publ. Eur. Commun. 165 p..
Wang, T., Camps-Arbestain, M., Hedley, M., Bishop, P., 2012. Predicting phosphorus bioavailability from high-ash biochars. Plant Soil 357, 173–187. https://doi.org/10.1007/s11104-012-1131-9.
Wang, C., Liu, D., Bai, E., 2018. Decreasing soil microbial diversity is associated with decreasing microbial biomass under nitrogen addition. Soil Biol. Biochem. https://doi.org/10.1016/j.soilbio.2018.02.003.
Wang, C., Luo, D., Zhang, X., Huang, R., Cao, Y., Liu, G., Zhang, Y., Wang, H., 2022. Biochar-based slow-release of fertilizers for sustainable agriculture: a mini review. Environ. Sci. Ecotechnol. https://doi.org/10.1016/j.ese.2022.100167.
White, P.J., Brown, P.H., 2010. Plant nutrition for sustainable development and global health. Ann. Bot. 105, 1073–1080. https://doi.org/10.1093/aob/mcq085.
Woolf, D., Amonette, J.E., Street-Perrott, F.A., Lehmann, J., Joseph, S., 2010. Sustainable biochar to mitigate global climate change. Nat. Commun. 1. https://doi.org/10.1038/Ncomms1053.
Xu, G., Sun, J.N., Shao, H.B., Chang, S.X., 2014. Biochar had effects on phosphorus sorption and desorption in three soils with differing acidity. Ecol. Eng. 62, 54–60. https://doi.org/10.1016/j.ecoleng.2013.10.027.
Yang, X., Xiong, J., Du, T., Ju, X., Gan, Y., Li, S., Xia, L., Shen, Y., Pacenka, S., Steenhuis, T.S., Siddique, K.H.M., Kang, S., Butterbach-Bahl, K., 2024. Diversifying crop rotation increases food production, reduces net greenhouse gas emissions and improves soil health. Nat. Commun. 15. https://doi.org/10.1038/s41467-023-44464-9.
Yao, Y., Gao, B., Zhang, M., Inyang, M., Zimmerman, A.R., 2012. Effect of biochar amendment on sorption and leaching of nitrate, ammonium, and phosphate in a sandy soil. Chemosphere 89, 1467–1471. https://doi.org/10.1016/j.chemosphere.2012.06.002.
Zayed, O., Hewedy, O.A., Abdelmoteleb, A., Ali, M., Youssef, M.S., Roumia, A.F., Seymour, D., Yuan, Z.C., 2023. Nitrogen journey in plants: from uptake to metabolism, stress response, and microbe interaction. Biomolecules. https://doi.org/10.3390/biom13101443.
Zhang, Q., Du, Z., Lou, Y., He, X., 2015. A one-year short-term biochar application improved carbon accumulation in large macroaggregate fractions. Catena 127, 26–31. https://doi.org/10.1016/j.catena.2014.12.009.
Zhang, G., Guo, X., Zhao, Z., He, Q., Wang, S., Zhu, Y., Yan, Y., Liu, X., Sun, K., Zhao, Y., Qian, T., 2016. Effects of biochars on the availability of heavy metals to ryegrass in an alkaline contaminated soil. Environ. Pollut. 218, 513–522. https://doi.org/10.1016/j.envpol.2016.07.031.
Zhao, L., Cao, X., Zheng, W., Scott, J.W., Sharma, B.K., Chen, X., 2016. Copyrolysis of biomass with phosphate fertilizers to improve biochar carbon retention, slow nutrient release, and stabilize heavy metals in soil. ACS Sustain. Chem. Eng. 4, 1630–1636. https://doi.org/10.1021/acssuschemeng.5b01570.